

# Quasiphase matching of second-harmonic generation in quantum cascade lasers by Stark shift of electronic resonances

Mikhail A. Belkin,<sup>a)</sup> Mariano Troccoli, Laurent Diehl, and Federico Capasso<sup>b)</sup>  
*Division of Engineering and Applied Sciences, Harvard University, Cambridge, Massachusetts 02138*

Alexey A. Belyanin<sup>c)</sup>  
*Department of Physics, Texas A&M University, College Station, Texas 77843*

Deborah L. Sivco and Alfred Y. Cho  
*Bell Laboratories, Lucent Technologies, Murray Hill, New Jersey 07974*

(Received 20 January 2006; accepted 29 March 2006; published online 16 May 2006)

We demonstrate a quasiphase matching scheme for second-harmonic generation in quantum cascade lasers with integrated resonant nonlinearity. Modulation of the nonlinear susceptibility is achieved by the periodic modulation of the bias voltage along the ridge waveguide leading to a periodic shift of electronic resonances and a change in the electron population in different energy levels. An up to tenfold enhancement of the conversion efficiency is observed. This technique is applicable to any resonant nonlinear optical process in quantum wells. © 2006 American Institute of Physics.  
 [DOI: 10.1063/1.2203938]

Nonlinear optical processes such as second-harmonic generation (SHG) and sum- and difference-frequency generation are extensively used in optics for frequency transformation. Quantum-well semiconductor nanostructures provide an opportunity to manipulate the nonlinear optical response by tailoring the energies and strengths of electronic transitions. Giant resonant electronic nonlinearities have been demonstrated with intersubband transitions in Refs. 1–4.

Recently it has been shown<sup>5–7</sup> that one can integrate quantum-well structures with giant nonlinear susceptibilities into the quantum cascade laser (QCL) active region. As a result, the laser radiation experiences nonlinear self-conversion into radiation at other frequencies via the interaction with the nonlinearity of the gain medium. This can be used to extend the spectral range available to QCL. To achieve high conversion efficiency in SHG and sum- and difference-frequency generation, a phase matching of the fundamental and generated waves is required.<sup>6–9</sup> Using modal phase matching, Malis *et al.* have recently achieved 2 mW of second-harmonic power output from QCL with 17 mW/W<sup>2</sup> conversion efficiency.<sup>9</sup> Here we demonstrate an alternative, quasiphase matching (QPM) scheme for SHG in QCL that utilizes unique properties of quantum-well nanostructures as artificial atoms with controllable electronic resonances.

The power of the beam at frequency  $2\omega$  generated in SHG scales as<sup>10</sup>

$$W_{2\omega} \propto \frac{|\chi^{(2)}|^2}{|\Delta\mathbf{k}|^2 + \alpha^2} W_{\omega}^2. \quad (1)$$

Here  $W_{\omega}$  and  $W_{2\omega}$  are the power of the beams at  $\omega$  and  $2\omega$ ,  $\chi^{(2)}$  is the nonlinear susceptibility of the medium, and  $\Delta\mathbf{k} = \mathbf{k}_{2\omega} - 2\mathbf{k}_{\omega}$  is the wave vector mismatch with  $k_{\omega} = n(\omega)\omega/c$ , where  $n(\omega)$  is the refractive index at frequency  $\omega$ . The parameter  $\alpha$  is related to the optical gain or losses of the medium at both fundamental and second-harmonic frequencies

and to inhomogeneous effects such as the random variations of  $\chi^{(2)}$ , random variations of  $\Delta\mathbf{k}$  in different parts of the sample, etc.<sup>11</sup> Here we assumed that the length of the sample is larger than  $1/\alpha$ . For efficient frequency conversion  $\Delta\mathbf{k}$  must be close to zero, the phase matching condition. Due to the materials dispersion, this condition is usually difficult to fulfill. Quasiphase matching utilizes the spatial modulation of the nonlinear susceptibility  $\chi^{(2)}$  with wave vector  $k_{\text{QPM}}$  to compensate the phase mismatch. For QPM Eq. (1) becomes<sup>11</sup>

$$W_{2\omega} \propto \frac{|\chi^{(2)}(k_{\text{QPM}})|^2}{(\Delta\mathbf{k} - k_{\text{QPM}})^2 + \alpha^2} W_{\omega}^2. \quad (2)$$

Here  $\chi^{(2)}(k_{\text{QPM}})$  is the Fourier component of  $\chi^{(2)}$  with the wave vector  $k_{\text{QPM}}$ . The QPM technique allows to match any frequencies and to have different modulations on the same device. However, typical methods to produce QPM materials require physical modification of the sample, such as periodic poling,<sup>12</sup> growth on patterned substrates,<sup>13</sup> wafer bonding,<sup>14</sup> etc. They all suffer from difficulty of structure fabrication.

Here we demonstrate a method to achieve QPM in QCL by spatial modulation of intersubband electronic resonances along the laser ridge utilizing the Stark effect. This can be done by spatially modulating the bias voltage using a metal grating for the top contact. This method does not require any physical modification of the QCL active region.

The nonlinear susceptibility of quantum-well structures depends on the energy level spacing and the electron population density in different energy states,<sup>7,11</sup>

$$\chi^{(2)} = N_e \frac{e^3}{\hbar^2} \sum_{n,n',nm} z_{nn'} z_{n'n} z_{nm} z_{nm} \times \left\{ \frac{1}{(2\omega - \omega_{n'n} + i\Gamma_{n'n})(\omega - \omega_{nm} + i\Gamma_{nm})} + \frac{1}{(2\omega + \omega_{n'n} + i\Gamma_{n'n})(\omega + \omega_{nm} + i\Gamma_{nm})} - \frac{1}{(2\omega - \omega_{n'nm} + i\Gamma_{n'nm})} \left[ \frac{1}{(\omega + \omega_{nm} + i\Gamma_{nm})} \right] \right\}$$

<sup>a)</sup>Electronic mail: mbelkin@deas.harvard.edu

<sup>b)</sup>Electronic mail: capasso@deas.harvard.edu

<sup>c)</sup>Electronic mail: belyanin@tamu.edu

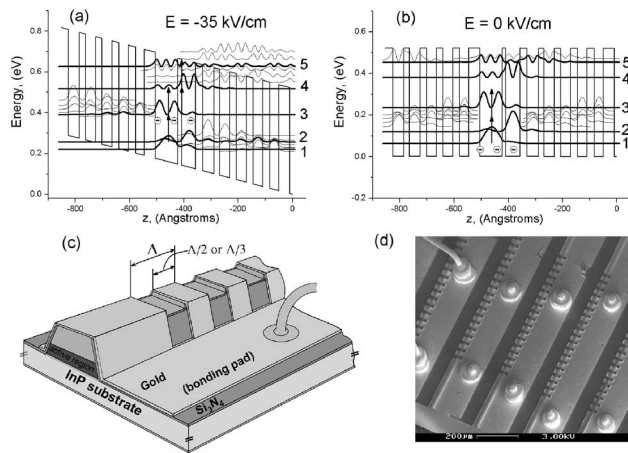


FIG. 1. (a) and (b) The structure of one active region sandwiched between two injector regions and the square of the magnitude of the electron wave functions of quantum cascade laser of design D2912 (Ref. 7) calculated for an applied electric field of (a) 35 kV/cm and (b) 0 kV/cm. (c) Schematics of the device with grating on top of the ridge. (d) The scanning electron microscopy (SEM) image of 12- $\mu\text{m}$ -ridge-width devices with 650- $\mu\text{m}$ -long grating on top of the ridges near one of the laser facets.

$$+ \frac{1}{(\omega - \omega_{n'n} + i\Gamma_{n'n})} \left. \right\} \rho_n. \quad (3)$$

Here  $N_e$  is the carrier density in the quantum wells,  $\rho_i$  is the population density in state  $i$ ,  $\omega_{ij}$ ,  $\Gamma_{ij}$ , and  $z_{ij}$  are the frequency, relaxation rate, and the transition dipole moment, respectively, for the transition between states  $i$  and  $j$ . Consider a QCL structure with integrated optical nonlinearity optimized for resonant SHG<sup>7</sup> [Figs. 1(a) and 1(b)]. Under the laser operating voltage [Fig. 1(a)], the energy levels 2–5 are Stark shifted to form transitions that are in resonance with both laser frequencies  $\omega$  and  $2\omega$ , the current is flowing across the active region and most of the electrons are in the upper laser state,  $\rho_3 \gg \rho_1$ ,  $\rho_2$ ,  $\rho_4$ , and  $\rho_5$ . Equation (3) then gives  $|\chi^{(2)}| \approx 2 \times 10^4$  pm/V.<sup>7</sup> On the other hand, for low bias voltage there is no current, electrons are mostly in state 1, and, without the Stark shift, the energy levels are no longer in resonance with  $\omega$  and  $2\omega$  [see Fig. 1(b)]. For zero bias Eq. (3) gives  $|\chi^{(2)}| \approx 10^3$  pm/V. Thus, by modulating the bias along the laser ridge, one can modulate the nonlinear susceptibility. Note that the distribution of the electric field and current in the QCL active region is a solution of the Poisson equation with the applied voltage providing the boundary conditions on top of the ridge. Typically one observes the “current spreading” effect.<sup>15</sup> The exact calculation of this effect is beyond the scope of this experimental letter. However, the calculations in Ref. 15 indicate that one should be able to achieve effective modulation of  $\chi^{(2)}$  in a QCL by modulating the bias voltage along the ridge.

To verify this experimentally, we processed the lasers from wafer D3045 [regrowth of D2912 (Ref. 7)]. The laser consists of 50 periods of active regions and injectors sandwiched between two waveguide layers of InGaAs, 600-nm-thick below and 400-nm-thick above, both  $n$  doped to  $10^{17}$  cm<sup>-3</sup>. The bottom waveguide cladding is provided by the InP substrate and the top cladding is made from an inner 2.1- $\mu\text{m}$ -thick AlInAs layer  $n$  doped to  $1 \times 10^{17}$  cm<sup>-3</sup>, an outer 0.4- $\mu\text{m}$ -thick AlInAs layer  $n$  doped to  $2 \times 10^{17}$  cm<sup>-3</sup>, and capped by a 0.35- $\mu\text{m}$ -thick InGaAs layer  $n$  doped to  $6.5 \times 10^{18}$  cm<sup>-3</sup>. The lasers were processed as deep-etched ridge waveguides with ridge widths 10–12  $\mu\text{m}$  (in the active

region). Laser bars with length  $\sim 2.5$  mm were cleaved from the processed chips. To achieve the modulation, we etched 0.75- $\mu\text{m}$ -deep, 650- $\mu\text{m}$ -long grating structures through the higher-doped layers on top of the ridges, near one of the laser facets, and placed gold contacts on top of the grating, as shown in Figs. 1(c) and 1(d). The rest of the ridge was left intact in effort to keep good laser performance. We estimated the phase mismatch for SHG in the lasers to be  $|\Delta\mathbf{k}| \sim 1500$ –1800 cm<sup>-1</sup>. Note that the periodic modulation of the waveguide structure may introduce additional QPM mechanisms through the modulation of the effective refractive indices of the modes or through the modulation of the mode profiles. We have considered these contributions and found them negligibly small. Two sets of samples were processed. In the first set, the samples had a ridge width of 12  $\mu\text{m}$  and the grating period was changed from 33 to 44  $\mu\text{m}$  ( $k_{\text{QPM}}$  changing from 1900 to 1400 cm<sup>-1</sup>); the current was injected through half of the grating period  $\Lambda$  [see Fig. 1(c)]. The samples in the second set had a ridge width of 10  $\mu\text{m}$  and the grating period was varied from 31 to 57  $\mu\text{m}$  ( $k_{\text{QPM}} = 2000$ –1100 cm<sup>-1</sup>); the current was injected through 1/3 of the grating period to compensate for the possible current spreading.<sup>15</sup> The lasers were operated at 77 K in pulsed mode with 125 ns current pulses with repetition rate of 80 kHz. The measurements were done with a calibrated thermopile detector for the fundamental light and a calibrated cooled InSb photovoltaic detector for SHG light.

The fundamental and SHG light output characteristics of the two typical lasers are presented in Fig. 2. The introduction of the grating structure on the ridge typically reduced the fundamental laser output power by approximately 30%. However, the amount of the emitted SHG light was higher for the devices with the grating. Plotted in Fig. 3 is the dependence of the conversion efficiency, defined as  $\eta = W_{2\omega}/W_\omega^2$ , on the grating period. The conversion efficiency peaks at  $2\pi/\Lambda$  around 1500 cm<sup>-1</sup> which agrees with the theoretically estimated phase mismatch  $|\Delta\mathbf{k}| \sim 1400$ –1800 cm<sup>-1</sup> confirming that we achieved QPM. Due to the significant scatter of the data, the exact positions of the conversion efficiency peaks are difficult to establish with accuracy better than 150 cm<sup>-1</sup>. The continuous line through the

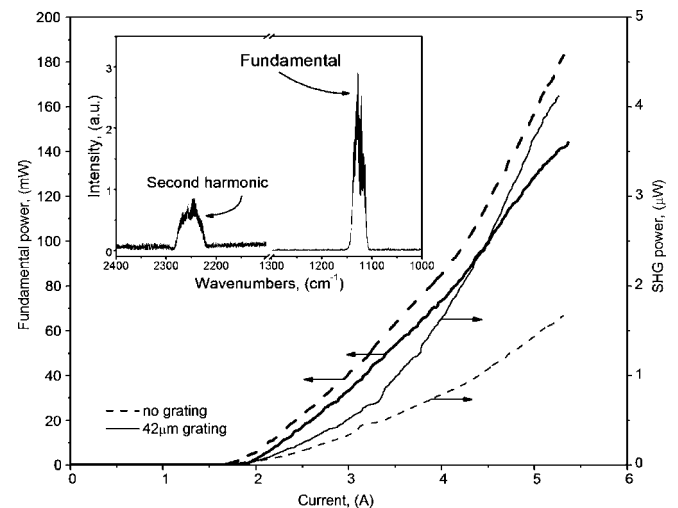


FIG. 2. Fundamental peak power output (left axis) and second-harmonic peak power output (right axis) vs current at 77 K for two representative 12- $\mu\text{m}$ -ridge-width devices with and without grating. Insert: representative spectra of fundamental and second-harmonic light from a device.

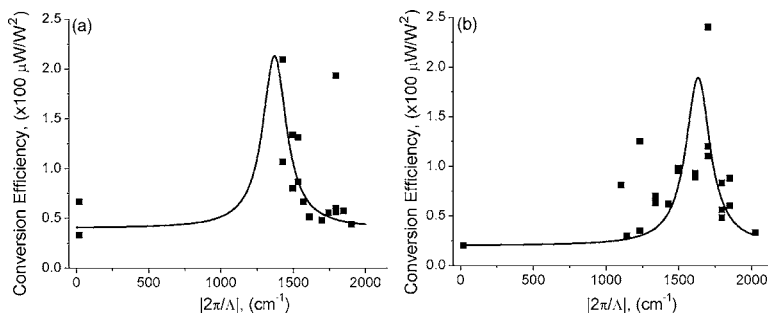


FIG. 3. Measured conversion efficiency as a function of contact grating period  $\Lambda$  for the samples with the ridge width of 12  $\mu\text{m}$  (a) and 10  $\mu\text{m}$  (b).

points is a function of the form  $1/[(k_{\text{QPM}} - \Delta k)^2 + \alpha^2]$ , expected from Eq. (2), with  $\alpha = 100 \text{ cm}^{-1}$  and  $\Delta k = 1370 \text{ cm}^{-1}$  [1630  $\text{cm}^{-1}$  for Fig. 3(b)]. The value of  $\alpha$  that determines the width of the peaks in Fig. 3 is significantly larger than  $\sim 20 \text{ cm}^{-1}$  estimated from the value of the waveguide losses due to resonant absorption of second-harmonic radiation. Large value of  $\alpha$  is likely due to the inhomogeneous effects such as ridge width nonuniformity and to the relatively short (650  $\mu\text{m}$ ) QPM modulation length. For an ideal  $L = 650 \mu\text{m}$  long QPM structure the half-width at half maximum of the peak of the conversion efficiency  $\eta(k_{\text{QPM}})$  is given as  $0.9\pi/L \approx 45 \text{ cm}^{-1}$ .<sup>11</sup> In addition, the wet-etch processing used to fabricate our devices results in 0.5 to 1  $\mu\text{m}$  ridge-width nonuniformity, leading  $\sim 50 \text{ cm}^{-1}$  variations in phase mismatch  $|\Delta k|$  in different parts of the ridge.<sup>8</sup> We believe that the ridge width and height variations between different devices are also the reason for the scatter of the data in Fig. 3. Overall we observed up to ten times improvement in the conversion efficiency in QPM samples. Assuming the current is injected through half of the grating period, there is no current spreading, and in the regions with no current  $\chi^{(2)} = 0.05\chi_{\text{max}}^{(2)}$ , where  $\chi_{\text{max}}^{(2)}$  is the nonlinearity under the laser operating condition, we obtain  $\chi^{(2)}(k_{\text{QPM}}) \approx \chi_{\text{max}}^{(2)}/\pi$ . A comparison of Eq. (1) with Eq. (2) shows that SHG conversion efficiency must improve by  $\sim 1/\pi^2 \times \Delta k^2/\alpha^2$ . Inserting  $\alpha = 100 \text{ cm}^{-1}$  and  $\Delta k = 1600 \text{ cm}^{-1}$  into this expression gives an improvement factor  $\approx 26$ . The experimentally measured value is approximately three times smaller, likely due to the current spreading effect that reduces the efficiency of the nonlinearity modulation. Further investigation is underway to improve the SHG conversion efficiency by the careful design of the contact grating, increasing the modulation length, and employing dry etching processing.

In summary, we have experimentally demonstrated a technique for QPM of SHG in QCL through the periodic Stark shift of the intersubband electronic resonances. The technique is easy to implement and does not require any modification of the QCL active region. It can also be used to improve the conversion efficiency of other nonlinear optical processes such as sum- and difference-frequency generation,

third-harmonic generation, and parametric frequency down-conversion in QCL and other semiconductor nanostructure devices based on a resonant electronic nonlinearity.

This work was supported by AFOSR under Contract No. FA9550-05-1-0435. The structures were processed in the Center for Nanoscale Science (CNS) in Harvard University. Harvard-CNS is a member of the National Nanotechnology Infrastructure Network. One of the authors (A.B.) acknowledges support from TAMU TITF Initiative, NSF through Grant Nos. ECS 0501537 and ECS 0547019, and AFOSR through Grant No. FA9550-05-1-0360. The authors would like to acknowledge helpful discussions with Oana Malis.

<sup>1</sup>M. K. Gurnick and T. A. DeTemple, IEEE J. Quantum Electron. **19**, 791 (1983).

<sup>2</sup>M. M. Fejer, S. J. B. Yoo, R. L. Byer, A. Harwit, and J. S. Harris, Phys. Rev. Lett. **62**, 1041 (1989).

<sup>3</sup>F. Capasso, C. Sirtori, and A. Y. Cho, IEEE J. Quantum Electron. **30**, 1313 (1994).

<sup>4</sup>E. Rosencher, A. Fiore, B. Vinter, V. Berger, Ph. Bois, and J. Nagle, Science **271**, 168 (1996).

<sup>5</sup>M. Troccoli, A. Belyanin, F. Capasso, E. Cubukcu, D. L. Sivco, and A. Y. Cho, Nature (London) **433**, 845 (2005).

<sup>6</sup>N. Owschimikow, C. Gmachl, A. Belyanin, V. Kocharovskiy, D. L. Sivco, R. Colombelli, F. Capasso, and A. Y. Cho, Phys. Rev. Lett. **90**, 043902 (2003).

<sup>7</sup>C. Gmachl, A. Belyanin, D. L. Sivco, M. L. Peabody, N. Owschimikow, A. M. Sergent, and F. Capasso, IEEE J. Quantum Electron. **39**, 1345 (2003).

<sup>8</sup>O. Malis, A. Belyanin, C. Gmachl, D. L. Sivco, M. L. Peabody, A. M. Sergent, and A. Y. Cho, Appl. Phys. Lett. **84**, 2721 (2004).

<sup>9</sup>O. Malis, A. Belyanin, D. L. Sivco, J. Chen, A. M. Sergent, C. Gmachl, and A. Y. Cho, Electron. Lett. **40**, 1586 (2004).

<sup>10</sup>Y. R. Shen, *The Principles of Nonlinear Optics* (Wiley, New York, 1984).

<sup>11</sup>M. M. Fejer, G. A. Magel, D. H. Jundt, and R. L. Byer, IEEE J. Quantum Electron. **28**, 2631 (1992).

<sup>12</sup>E. J. Lim, H. M. Hertz, M. L. Bortz, and M. M. Fejer, Appl. Phys. Lett. **59**, 2207 (1991).

<sup>13</sup>L. A. Eyres, P. J. Tourreau, T. J. Pinguet, C. B. Ebert, J. S. Harris, M. M. Fejer, L. Becouarn, B. Gerard, and E. Lallier, Appl. Phys. Lett. **79**, 904 (2001).

<sup>14</sup>L. Becouarn, E. Lallier, M. Brevignon, and J. Lehoux, Opt. Lett. **23**, 1508 (1998).

<sup>15</sup>Cyrille Becker and Carlo Sirtori, J. Appl. Phys. **90**, 1688 (2001).